(Proposal to Jefferson Lab PAC 31)

Measurement of non-pole backgrounds in the extraction of the charged pion form factor

December 12, 2006

H. Avakian, P. Bosted, H. Fenker, R. Feuerbach, D. Gaskell (co-spokesperson)
D. Higinbotham, T. Horn (co-spokesperson), M. Jones, D. Mack
Jefferson Lab, Newport News, VA 23606

C. Butuceanu, G. M. Huber (co-spokesperson), G.J. Lolos
University of Regina, Regina, SK S4S-0A2 Canada

A. J. Sarty
Saint Mary's University, Halifax, Nova Scotia B3H 3C3 Canada

W. Boeglin, P. Markowitz, J. Reinhold
Florida International University, Miami, FL 33199

D. Dutta
Mississippi State University, Mississippi State, MS 39762-5167

V. Koubarovski, P. Stoler
Rensselaer Polytechnic Institute, Troy, NY 12180-3590

A. Asaturyan, A. Mkrtchyan, H. Mkrtchyan, V. Tadevosyan
Yerevan Physics Institute, Yerevan, Armenia

E. Brash
Christopher Newport University, Newport News, Virginia

A. Aniol
California State University Los Angeles, Los Angeles, California 90032

J. Calarco
University of New Hampshire

P. King, J. Roche
Ohio University, Athens, OH 45701

Purpose

The purpose of this experiment is to perform measurements of the longitudinal and transverse cross sections for exclusive $\mathrm{H}(\vec{e}, e'\vec{p})\pi^0$ data above the resonance region at Q^2=2.45 GeV^2, 3.1 GeV^2 and 3.8 GeV^2. Since the π^0 cross section does not have a large pole contribution it should be sensitive to non-pole contributions to the π^+ cross section, which is important for the extraction of F_π from π^+ electroproduction data. These data will provide one of the most stringent tests on

the size of the non-pole backgrounds for $-t_{min} > 0.2$, which may place a constraint on the value of $-t_{min}$ for which one can reliably extract the pion charge form factor.

The proposed measurement will be the first opportunity to access the separated longitudinal π^0 cross section at large $Q^2 >$ above the resonance region.

The simultaneous measurement of the η reaction channel allows for the determination of the π^0/η cross section ratio to test various factorization theorems.

I. SCIENTIFIC BACKGROUND

A. Introduction

By performing a measurement constraining non-pole backgrounds in the extraction of the pion form factor, F_π, we have the unique opportunity to improve the kinematic reach of one of the highest priority programs for the Jefferson Lab 12 GeV program, the precise determination of the pion form factor, F_π. This measurement is of particular interest in our understanding of hadronic structure in the transition region from non-perturbative to perturbative degrees of freedom in the Q^2 regime greater than 6 GeV^2. The extraction of F_π from pion electroproduction data relies on pion pole dominance, and to avoid possibly large non-pole contributions, experiments are typically limited to low values of $-t$, which in turn limits the accessible Q^2 range.

The goal of this proposal is to constrain the size of the non-pole contributions in charged pion electroprodution by making a systematic measurement of the π^0 longitudinal cross section. One study predicts that the perturbative QCD longitudinal cross section is comparable in size for both the π^+ and π^0 electroproduction cross sections [1]. This is different from the simpler interpretation that $\sigma_L \approx 0$ for neutral pion electroproduction, since the pion exchange diagam does not contribute. Thus, a significant longitudinal response in forward π^0 electroproduction may be indicative of non-pole contributions in forward charged pion electroproduction. In fact, much can be learned about our understanding of π^0 processes as the extraction of σ_L allows us to test for the first time the contribution of the longitudinal responses to the unseparated cross section.

We propose to make measurements of forward π^0 electroproduction by detecting backward protons. We will extract the ratio of longitudinal (σ_L) to transverse (σ_T) cross sections via recoil polarimetry techniques. Simultaneous measurement of the unseparated cross section will allow for the extraction of σ_L.

B. Contributions from the pion pole

The lowest order processes contributing to pion electroproduction are the meson and nucleon pole diagrams. In the limit of pole dominance, the cross section can be directly related to the pion form factor. However, other processes may contribute, complicating the extraction of F_π using π^+ production. In this simple pole dominance picture F_π can be related to the longitudinal cross section,

$$\sigma_L \sim \frac{-tQ^2}{(t-m_\pi^2)^2} g^2_{\pi NN}(t) F^2_\pi(Q^2), \tag{1}$$

where $-t$ is the four-momentum transfer to the nucleon, Q^2 is the invariant mass of the exchanged virtual photon, and $g^2_{\pi NN}$ is the probability for finding a virtual photon inside the nucleon of a particular momentum.

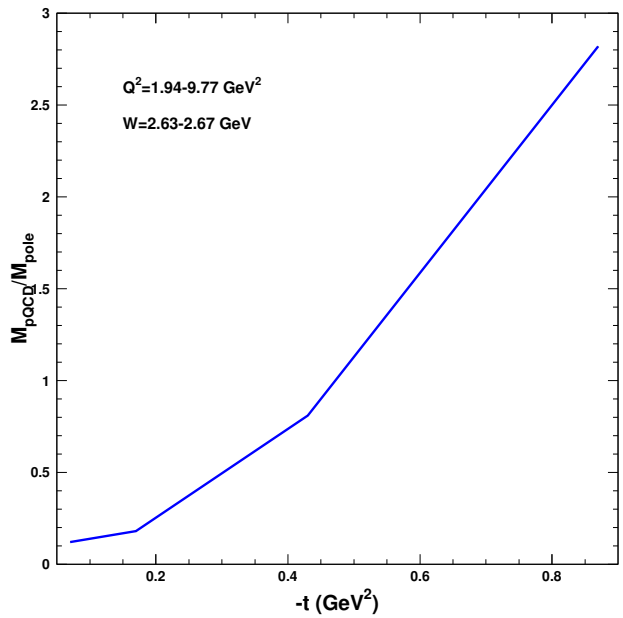

FIG. 1: *The ratio of M_{pQCD}/M_{pole} from reference [1] for several high Q^2 data points from reference [2]. The background to pole ratio rises significantly at higher $-t$, complicating the extraction of F_π in these kinematics.*

At moderate and high momentum transfers, pion electroproduction can be expressed in terms of pQCD quark gluon diagrams, which constitute a competing reaction contribution to the pion pole diagram. These diagrams are thought to be the main source of π^0 production in the absence of a major pole contribution [1].

The size of competing non-pole contributions to the forward pion electroproduction cross section at large values of Q^2 has been controversial for a long time. This is in part due to the lack of data in this region complicating theoretical estimates. Carlson and Milana raised the issue that the presence of non-pole processes obscures the extraction of F_π and they pointed out that the contribution of non-leading diagrams increases significantly at large values of $-t$ [1]. Figure 1 illustrates the background estimate for several high Q^2 data points from reference [2]. One can see that the ratio of the background to pole amplitude, M_{pQCD}/M_{pole}, rises significantly once $-t$ reaches a value of 0.2 GeV^2. The problem of such non-pole contributions was re-visited nine years later by Mankiewicz, Piller and Radyushkin [4]. There, pseudoscalar and pseudovector pion production were expressed in terms of quark double distribution functions of the nucleon, and the optimal region for $-t$ was confirmed to be consistent with the one determined earlier by Carlson and Milana. As a result, the interpretation of experimental data is widely considered reliable only below $-t_{min} \approx 0.2$ GeV^2. This places a severe kinematic constraint on F_π measurements, and is the primary reason we are limited to $Q^2 \approx 2.5$ GeV^2 at JLab (at 6 GeV).

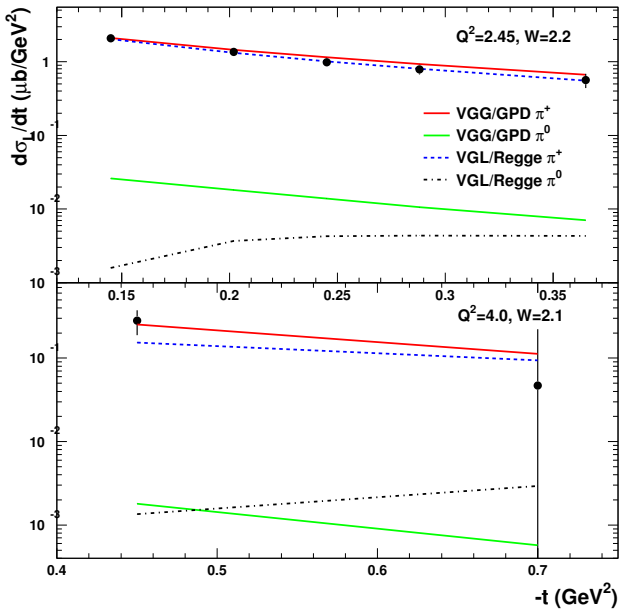

FIG. 2: *VGL Regge model [5] and VGG GPD [6] predictions for the longitudinal cross sections at two values of Q^2 for both charged and neutral pion production. The data points are from the recently completed analysis of the E01-004 (F_π-2) experiment [7].*

The poor quality of experimental data for F_π at high Q^2, combined with only few theoretical studies, make it clear that it is difficult to construct a satisfactory upper bound on the value of $-t$ one can use in the extraction of F_π. In reference [2], Bebek et al. present values for F_π extracted from pion electroproduction data in the region above Q^2=3 GeV^2. In these experiments the values of $-t_{min}$ were much larger than 0.2 GeV^2, and the reliability of the F_π extraction was questioned due to the estimated contribution of non-pole processes. Note that the size of these processes has not been explicitly measured to date.

In order to quantify the impact of the non-pole contributions one needs to use a model relating the π^0 and π^+ cross sections. Theoretical models based on Regge theory are available for the description of non-pole contributions in pion electroproduction data. A Regge model developed by Vanderhaeghen, Guidal and Laget (VGL, [5]) models the exchange of ρ and π- like particles by replacing the standard Feynman propagators, $1/(t-m^2)$, with Regge propagators that account for the exchange of a family of particles with the same internal quantum numbers.

The interpretation of non-pole contributions in the Regge framework is helped by the negligible influence of the ρ trajectory on the longitudinal π^+ cross section. While the π^+ cross section is dominated by the pion trajectory, it also includes some contribution from the ρ trajectory (although these are vanishingly small in this model). In the context of the Regge model, the π^0 longitudinal cross section is relatively small. A measurement of significant longitudinal strength

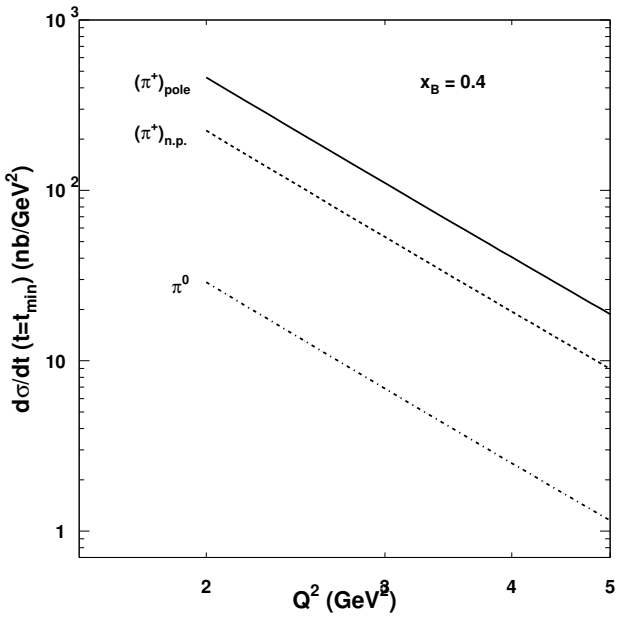

FIG. 3: *Contribution of the pion pole to the π^+ cross section in the VGG/GPD framework [6]. Here a running coupling constant on the scale Λ_{QCD} was used. For the π^+ channel the pion pole contribution (solid line) is shown separately from the $\tilde{H}$ contribution (dashed line).*

would imply a larger role for the ρ or ω trajectory than originally thought. Note that the theoretical uncertainty for the individual contribution to the longitudinal cross section is quite large [5, 6]. The relative order of magnitude between π^+ and π^0 cross sections as predicted by the Regge model is illustrated in Figure 2.

Non-pole contributions can also be interpreted using Generalized Parton Distributions (GPDs). GPDs are universal objects that describe the structure of the nucleon in a process-independent way, and combine the characteristics of parton distributions with those of elastic form factors. In the case of π^+ and π^0 production the amplitudes involve only the axial GPD's, $\tilde{H}$ and $\tilde{E}$, whose first moments can be related to the axial and pseudoscalar form factors [8].

$$\int_{-1}^{1} dx \tilde{H}(x;t) = G_A(t),$$
$$\int_{-1}^{1} dx \tilde{E}(x;t) = G_P(t). \tag{2}$$

In the GPD framework information on non-pole contributions can be obtained by comparing the π^+ and π^0 production amplitudes. The pion production amplitude for a virtual photon can be written (schematically), [9],

$$M_\pi^L \sim (A_{\pi N} + B_{\pi N}). \tag{3}$$

For π^0 production, the amplitudes A and B are [10, 11],

$$\begin{aligned} A_{\pi^0 p} &\sim (e_u \tilde{H}^u - e_d \tilde{H}^d), \\ B_{\pi^0 p} &\sim (e_u \tilde{E}^u - e_d \tilde{E}^d), \end{aligned} \tag{4}$$

and for π^+ production, the amplitudes A and B are given by [4, 12],

$$\begin{aligned} A_{\pi^+ p} &\sim (\tilde{H}^u - \tilde{H}^d)(e_u + e_d), \\ B_{\pi^+ p} &\sim (\tilde{E}^u - \tilde{E}^d)(e_u + e_d). \end{aligned} \tag{5}$$

In the limit $t \to m_\pi^2$ the π^+ production amplitude contains an additional pion pole contribution. The pion pole appears as a strong singularity in the function $\tilde{E}^u - \tilde{E}^d$, and is generally assumed to dominate over the regular part of the amplitude. By charge conjugation invariance the pion pole is absent in the π^0 production amplitude. Figure 3 shows the pion pole contribution and the regular contribution to the π^+ channel as predicted by the GPD model by Vanderhaeghen, Guichon and Guidal[6].

Besides π^0 electroproduction, one can also study some interesting relations between the ratio of cross sections for π^0 and η production. These follow from the universality of the GPDs [13], and provide a unique way to probe the ratio of $\Delta d/\Delta u$ using an unpolarized target.

In the limit of SU(3) flavor symmetry and neglecting the effects of the U(1) axial QCD anomaly, the ratio of π^0:η cross sections can be written,

$$\pi^0 : \eta = \frac{1}{2}\left(\frac{2}{3}\Delta u + \frac{1}{3}\Delta d\right)^2 : \frac{1}{6}\left(\frac{2}{3}\Delta u - \frac{1}{3}\Delta d + \frac{2}{3}\Delta s\right)^2 \tag{6}$$

where Δu, Δ d and Δ s are the polarized quark densities in the proton. Assuming Δ d $\approx$ -Δ u and Δ s=0, the cross section ratio was predicted to be π^0:η= 1:3 [14]. If one takes the effect of SU(3) symmetry breaking and the U(1) anomaly into account, this prediction changes to 1:4.8. The enhancement of the η fraction was attributed to the enhancement of the η coupling with u and d quarks [13]. It should be emphasized that GPD related studies of π^0 and η electroproduction rely on assumptions of the dominance of the longitudinal cross section, or the explicit isolation of the longitudinal channel.

C. Previous Data and Analysis

Previous exclusive π^0 electroproduction data above the resonance region are available from Jefferson Lab experiments such as Hall B experiments e1-6 and Hall A experiments E00-110 [16]. One of the goals of the former measurements was to study the onset of the partonic reaction mechanism. The differential cross section for meson production was measured in a kinematic region of W=2.1-2.7 GeV covering a range in Q^2 of 1 to 5 GeV^2 and momentum transfers $-t$=0.1-5 (GeV/c)^2. Preliminary results for the η production cross section can be found in reference [17].

Though the extraction of the interference terms can be achieved using the CLAS acceptance, the measured cross sections cannot be separated into the components corresponding to longitudinally and transversely polarized photons without assumptions on each contribution. Thus, additional information on the relative size of longitudinal and transverse components is of interest for further interpretation of these existing data from Hall B. The kinematic reach of e1-6 overlaps with all of the kinematics proposed for this measurement. The main focus of experiment E00-110 was the study of the Deeply Virtual Compton Scattering process at x_B=0.35 and covering a range in Q^2 from 1.4 to 2.3 GeV^2. These data include the π^0 production channel whose analysis is presently underway. Note however that these data cannot be separated into longitudinal and transverse contributions.

The ratio of the components of the cross sections may also be of interest to the study of exclusive π^0 cross sections with CLAS12 [17]. The main focus of the experiment is the comprehensive study of exclusive π^0 and η production including the detailed investigation of factorization predictions. Part of the measurement is dedicated to the study of π^0 separated cross sections. However, depending on the absolute size of e.g. σ_L a detailed study of the separated π^0 cross section using CLAS12 alone may be complicated. If σ_L is relatively small, absolute measurements of the separated cross sections may require additional information from double-arm spectrometer setups like the ones in Hall A and Hall C. Thus, the separated results from the proposed measurement may influence part of the final design of the 12 GeV π^0 program.

Experiments using the recoil polarization technique detecting a forward proton were performed at JLab in Hall A ([18, 19]) as well as at Mainz [20]. The main goal of experiment E93-103 was the study of the quadrupole strength around the Δ resonance using recoil polarization at Q^2=1.0 GeV^2. The comprehensive angular coverage included data sensitive to the longitudinal polarization of the photon. A separation of the longitudinal π^0 cross section was attempted, but currently no official publication of these data is available. Most of the earlier exclusive π^0 electroproduction data including [21] are limited to center of mass energies in the resonance region and cannot be easily separated due to kinematic constraints. Therefore, though demonstrating the feasibility and success of the recoil polarization method, these data cannot provide information on the contribution of non-pole contributions.

D. Impact on Existing and Future F_π Measurements

One reason for focusing on pion electroproduction data above the resonance region is to acquire π^0 production data in a kinematic region of existing F_π data from Jefferson lab obtained from forward charged pion electroproduction [22, 23]. The E01-004 (F_π-2, [7, 23]) experiment measured F_π up to Q^2=2.45 GeV^2 building on earlier high precision data from experiment E93-021 (F_π-1, [22, 24]) obtained for values of Q^2 between 0.6 and 1.6 GeV^2. Additional pion electroproduction data allowing for the extraction of F_π were taken during E01-107 (πCT) at Q^2=2.15 GeV^2 and

Q^2=4.0 GeV^2. The experimental cross section data are generally well described by modern calculations based on Regge theory like the one by Vanderhaeghen, Guidal and Laget (VGl). As shown in a series of articles [5] these predictions also agree relatively well with the available photoproduction data at low Q^2 for both π^+ and π^0 production. An improved calculation for π^0 electroproduction is currently underway [26].

The extension of the F_π measurement to Q^2=6 GeV^2 was recently approved for the Jefferson Lab 12 GeV Upgrade [27]. There, the maximum value of Q^2 was selected to avoid large non-pole contributions for $-t_{\rm min} < 0.2$ GeV^2. The proposed measurement would use the most directly accessible experimental method to constrain the size of non-pole background, which will also constrain the largest value of $t_{\rm min}$ for which one may extract a reliable value of F_π at even larger Q^2. In particular, comparison to the Q^2=4 GeV^2 data with $-t_{min} \approx 0.4$ is especially interesting. **If non-pole backgrounds are smaller than anticipated, this would dramatically increase the kinematic range accessible in a 12 GeV F_π experiment.**

II. EXPERIMENTAL METHOD

In this experiment we will measure separated cross sections for the p$(\vec{e}, e'\vec{p})\pi^0$ reaction using the recoil polarization technique in parallel kinematics. This approach is different from the Rosenbluth separation technique, which is typically used to separate σ_L and σ_T from pion electroproduction data. There, the systematic uncertainty due to differences in acceptance depends significantly on R=σ_L/σ_T. For most π^+ production measurements this parameter is large making L/T separations relatively straightforward. On the other hand, if the longitudinal piece becomes very small, the resulting rapid increase in the systematic uncertainty makes a meaningful L/T separation via Rosenbluth separation quite challenging. The recoil polarization technique in parallel kinematics offers an alternative way to extract the longitudinal contribution to the unseparated cross section without the adverse increased sensitivity to the acceptance.

The kinematics of the p$(\vec{e}, e'\vec{p})\pi^0$ reaction are illustrated in Figure 4. The incident electron with four momentum k=(ϵ_k,$\mathbf{k}$) scatters through an angle θ_e to a final four momentum q=(ω,$\mathbf{q}$). The electron scattering plane is defined by the three momenta $\mathbf{k}$ and $\mathbf{k}'$ and also includes the exchanged virtual photon three momentum transfer $\mathbf{q}$. The virtual photon is absorbed by the target nucleus eliminating a proton with four-momentum p'=($E(p'$,$\mathbf{p}$)), where $\mathbf{p}$ is oriented relative to the scattering plane by a polar angle θ_{pq} and an azimuthal angle ϕ_{pq}. The recoil of the residual system is given by four-momentum transfer p_r=$q - p'$, where the three-momenta $\mathbf{p}$ and $\mathbf{p_r}$ define the reaction/hadronic plane. The coordinate system for the recoil nucleon polarization are defined follows. The unit vectors $\hat{n}, \hat{l}$, and $\hat{t}$ form a right-handed coordinate system. For parallel kinematics the components of the recoil nucleon polarization are defined relative to the electron scattering plane where $\hat{l} = \hat{q}$ is defined in the photon direction, $\hat{n} = \hat{k_i} \times \hat{k_f}$ is normal to the electron scattering plane, and $\hat{t} = \hat{n} \times \hat{l}$ is transverse.

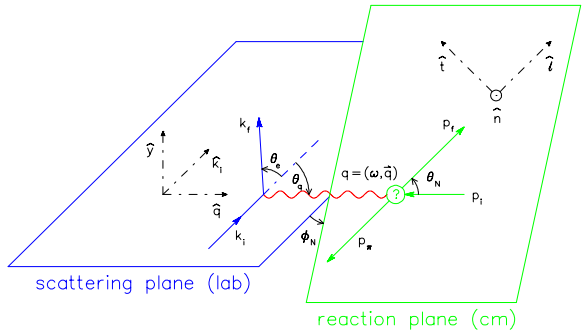

FIG. 4: *Kinematics of the $p(\vec{e}, e'\vec{p})\pi^0$ reaction and polarization basis vectors. Figure from reference [18]*

The differential pion electroproduction cross section can be written as the product of a virtual photon flux factor and a virtual photon cross section. Without target or recoil polarization, the virtual photoproduction cross section can written [28],

$$2\pi\frac{d^2\sigma}{dtd\phi} = \frac{d\sigma_T}{dt} + \epsilon\frac{d\sigma_L}{dt} + \sqrt{2\epsilon(1+\epsilon)}\frac{d\sigma_{LT}}{dt}cos\phi + \epsilon\frac{d\sigma_{TT}}{dt}cos2\phi. + h\sqrt{2\epsilon(1-\epsilon)}\sigma_{LT'}sin\phi \qquad (7)$$

where σ_L, σ_T, σ_{LT} and σ_{TT} denote the cross sections for the various polarization states of the virtual photon. Here, $\epsilon = \left(1 + 2\frac{|\mathbf{q^2}|}{Q^2}\tan^2\frac{\theta}{2}\right)^{-1}$ is the virtual photon polarization, where $\mathbf{q^2}$ is the square of the three-momentum transferred to the nucleon and θ is the electron scattering angle, and h is the longitudinal electron beam polarization. Along the direction of the virtual photon, the interference terms (LT and TT) go to zero, and in addition if one integrates over ϕ_{pq} for values of θ_{pq} >0 these terms will also vanish.

The individual components in equation 7 are typically determined from a fit to the ϕ dependence of the measured cross sections, $\frac{d^2\sigma}{dtd\phi}$, at two values of ϵ (Rosenbluth technique). This method requires measurements for at least two kinematics of quite different acceptances. If the longitudinal contribution becomes small the systematic uncertainty due to differences in the acceptance can become quite large making a meaningful measurement difficult.

As an alternative, for the special case of parallel kinematics, polarization observables can be used to separate longitudinal and transverse amplitudes without the traditional Rosenbluth separation method [29, 30]. The general cross section of the $p(\vec{e}, e'\vec{p})\pi^0$ reaction consists of eighteen structure functions [28, 31]. However, in parallel kinematics, where the proton is detected along the momentum transfer, the components of the proton recoil polarization simplify to [32],

$$\sigma_0 P_x = hc^- \frac{R^t_{LT'}}{R_T + \epsilon R_L} \qquad (8a)$$

$$\sigma_0 P_y = c^+ \frac{R^n_{LT}}{R_T + \epsilon R_L} \qquad (8b)$$

$$\sigma_0 P_z = hc^0 \frac{R^l_{TT'}}{R_T + \epsilon R_L} \qquad (8c)$$

where $\sigma_0 = \sigma_T + \epsilon\sigma_L$ is the proton polarization independent differential cross section, R^K_i are the

structure functions in the notation from reference [28], and the kinematic factors are given by $c_{\pm} = \sqrt{2\epsilon(1 \pm \epsilon)}$, and $c_0 = \sqrt{1-\epsilon^2}$.

The structure functions in equation 8 can be decomposed further into six independent helicity amplitudes [33, 34], which can be written (in parallel kinematics only) [29],

$$\begin{aligned} R_T &= \frac{1}{2}|H_4|^2 \\ R_L &= |H_6|^2 \\ R^t_{LT'} &= -\frac{1}{\sqrt{2}} Re(H_6^* H_4) \\ R^n_{LT} &= \frac{1}{\sqrt{2}} Im(H_6^* H_4) \\ R^l_{TT'} &= \frac{1}{2}|H_4|^2 \end{aligned} \tag{9}$$

$R^t_{LT'}$ and R^n_{LT} denote the real and imaginary parts of the same complex interference term. Note especially the equality of $R^l_{TT'}$ and R_T in parallel kinematics.

Using equation 8c and $R^l_{TT'}$=R_T, the ratio between longitudinal and transverse contributions to the differential cross section may be expressed,

$$R = \frac{\sigma_L}{\sigma_T} = \frac{1}{\epsilon}\left(\frac{1}{\chi_z} - 1\right), \tag{10}$$

where $\chi_z = \frac{P_z}{h\sqrt{1-\epsilon^2}}$ is the reduced polarization. Note that the reduced polarization is related to the unseparated cross section, σ_0,

$$\chi_z^2 = \frac{\sigma_T^2}{(\sigma_T + \epsilon\sigma_L)^2}. \tag{11}$$

which $\approx$1 in the limit of small σ_L. The longitudinal cross section can be obtained from the unpolarized cross section, σ_0, and the longitudinal to transverse ratio from equation 10.

$$\sigma_L = \frac{\sigma_0}{\left(\frac{1}{R} + \epsilon\right)}. \tag{12}$$

III. PROPOSED KINEMATICS

In this experiment, we propose to make coincidence measurements between recoil protons in the hadron arm of the Hall A spectrometers and electrons in the electron arm. The polarization of the recoil protons will be measured with the focal plane polarimeter in the left HRS. The high luminosity HRS spectrometer system is well-suited for such a measurement providing the high statistics needed for a recoil polarization measurement with θ_{pq} near zero degrees. The Hall A spectrometers easily provide the necessary time delay for detecting the slow hadron in coincidence with the scattered electron without any major modifications to the data aqcuisition setup.

Running this experiment in Hall C is in principle feasible. Though the angular acceptance of the SOS limits the accessible kinematics, the experiment could be done by detecting the electron

in the SOS and the recoiling proton in the HMS. The main constraint remains the re-design of the trigger and the data aquisition system to allow for detecting slow hadrons in coincidence. A trigger for the HMS could be designed by allowing for extra coincidence timing delays up to 100 ns. The use of the HRSs in Hall A is proposed here as the current data acquisition system can already accomodate this measurement without a re-design.

Table I shows the kinematic settings proposed for this experiment. The contribution of non-pole backgrounds will be examined at several Q^2 points, and relatively large values of $-t$. The data will be taken in parallel kinematics, and the separation of the components of the cross section will be achieved via recoil polarization observables. All data are acquired in parallel kinematics, which greatly simplifies the number of polarization variables.

The data points in Table I allow for a scan of the Q^2 dependence of the cross section at constant center of mass energy. In order to examine the $-t$ dependence of $\sigma_T + \epsilon\sigma_L$ we are planning to take data to the left and right to the $\mathbf{q}$ vector at Q^2=3.10 GeV^2. The points at Q^2=2.45 and 3.80 GeV^2 are similar to the kinematics from previous pion electroproduction measurements at JLab [23, 25] and allow for direct comparison with the π^+ cross sections. The ratio of the π^0 to η cross section, which is a by-product of this measurement, will be studied at Q^2=3.1 GeV^2.

We expect that the spectrometers coincidence timing can be set for hadron momenta as low as 450 MeV, which corresponds to a timing delay of $\approx$ 100 ns relative to the coincident electron. However, we conservatively chose the central proton momentum for our lowest kinematic point to be $\approx$ 30% above this limit to alleviate potential issues with such long delay times. The hadron angles range between 15.6 and 20.4 degrees with the minimum opening angles much greater than the 25.0 degree hardware limit. Thus, we will not require the use of the septum magnets [35]. We propose to take data at a single beam energy of E_e=5.75 GeV. The values of ϵ are the largest possible virtual photon polarizations for a given kinematic setting. The longitudinal to transverse π^0 cross section ratios will be extracted from the polarization observables, while simultaneous measurement of $\sigma_T + \epsilon\sigma_L$ will allow the extraction of the contribution of σ_L.

Figure 5 shows simulated Q^2=2.45, 3.1, and 3.8 GeV^2 data for electrons in the right HRS and the recoiling proton detected in the left HRS. The acceptance is asymmetric and is limited to a rectangular shape as expected for constant $\mathbf{q}$ kinematics. Cuts will be placed to equalize the $\phi - \theta$ range measured along the virtual photon direction. The angular distribution ranges between 2 and 4 degrees and is adequate to obtain the cross section in parallel kinematics.

A. Particle Identification

The HRS spectrometers will be configured for hadron detection in the left spectrometer and electron detection in the right spectrometer. The hadron arm will be equipped with the FPP to identify the recoiling proton.

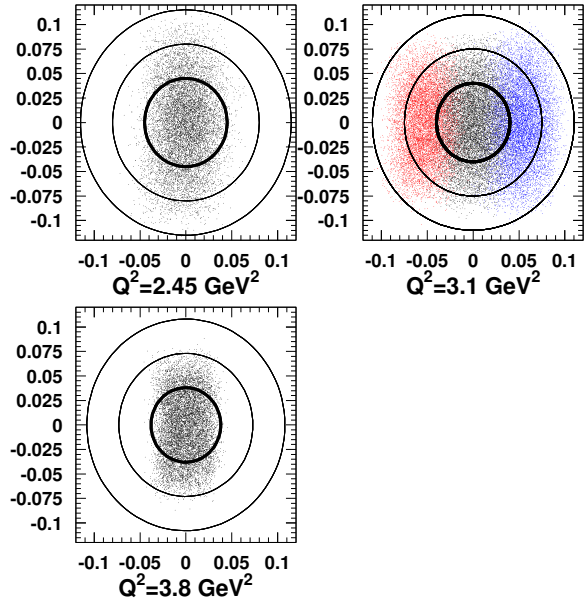

FIG. 5: *Simulated θ_{pq} (radial coordinate) vs. azimuthal angle ϕ_{pq} for the proposed kinematic points. Each radial division corresponds to θ_{pq}=0.5 degrees. The parallel cut is indicated by the inner circle.*

TABLE I: *Kinematic settings for $p(\vec{e}, e'\vec{p})$ π^0 experiment. The points at Q^2=2.45 and 3.8 GeV^2 overlap with the values for t_{min} for particular t-bins from the F_π-2 and the πCT experiments. Note that all settings are for parallel kinematics only.*

W (GeV)	Q^2 (GeV^2)	E_e (GeV)	E'_e (GeV)	θ_e (deg)	ϵ	p_p (GeV)	θ_p (deg)	$-t_{min}$ (GeV/c)^2	x
1.90	2.45	5.75	2.990	21.76	0.77	0.585	20.44	0.314	0.47
2.00	3.10	5.75	2.436	27.21	0.65	0.641	17.26	0.372	0.50
2.00	3.80	5.75	2.063	32.88	0.56	0.751	15.57	0.494	0.55

B. FPP

In the experiment we will measure the polarization of low energy protons with momenta between 585 and 751 MeV/c. The analyzing power for most of the proposed kinematics is large. It has been measured in the summer of 2006 by Hall A experiment E05-103(LEDEX, [39, 40]), and it is a well known function of the proton energy. The results are largely consistent with the McNaughton parameterization from reference [41]. For the rate estimations we have used the preliminary results from this recent low energy Hall A measurement. Table II summarizes the polarimeter and spin-transport characteristic parameters.

TABLE II: *Assumed FPP and spin transport parameters. The values for the analyzing power and efficiency are taken from LEDEX [40]. These values interpolated for the proposed data points are listed in the last column for reference. The* t_C *indicates the analyzer thickness (carbon door thickness) in mm. The effect of multiple scattering increases at momenta* < 500 *MeV requiring a smaller door thickness than the one used at larger proton momenta. In LEDEX carbon analyzer thicknesses of 19 mm were used for proton momenta* < 580 *MeV. The thickness at larger momenta ranged between 57 and 95 mm. For the proposed measurement we will use door thicknesses similar to the ones from LEDEX.*

W (GeV)	Q^2 (GeV^2)	p_p (GeV)	χ (deg)	t_C (mm)	$< \varepsilon \bar{A}_C^2 >$
1.90	2.45	0.585	94.9	38	0.00695
2.00	3.10	0.641	97.6	38	0.01267
2.00	3.80	0.751	103.2	38	0.01054

C. Backgrounds

Singles rates from (e, π^+) and (e, K^+) can result in accidental coincidences which are a source of background for the measurement. However, the low energy backward detection of the electroproduced proton is nearly background free at Q^2=2.45 GeV^2. At forward angles the electroproduction protons have a lower momentum than any particle from the hydrogen target. While higher momentum pions and kaons are kinematically allowed at backward angles the separation of pions and protons would not pose a problem. If there are pions, they can be eliminated from the event sample using time of flight cuts. For example, 500 MeV protons (pions) have velocities of β=0.47 (0.96), which are well separated compared to the expected resolution.

The singles rates into both spectrometers were estimated and are summarized in Table IV. For the electron rates, the QFS program by O'Connell and Lightbody [42] was used, while the hadron rates were estimated uing a fit to experimental pion and nucleon photoproduction at higher energies [43]. In calculating the accidental coincidence rates, the hadron trigger rate was taken to be equal to the raw trigger rate, so no distinction between pions, kaons and protons was made in the trigger. The online π^- rejection rate was assumed to be 1:100, which is achievable with the Hall A detector packages [35]. The coincidence resolving time was taken to be 2 ns. One can see that the accidental coincidence rates are not a significant source of background. Placing cuts on the missing mass will reduce the accidental background to just a few percent of the real coincidence rate.

The unobserved π^0 will be identified via the missing mass, which is reconstructed from the final electron and proton four-momenta. Cutting on the missing mass will reduce both random coincidences and background from events with larger inelasticity than $\mathrm{p}(e, e'p)\pi^0$. For example, events from the $\mathrm{p}(e, e'p)\eta$ reaction are effectively removed. The missing mass acceptance is illustrated in Figure 6 and has a missing mass squared resolution which varies between 0.10 and 0.14

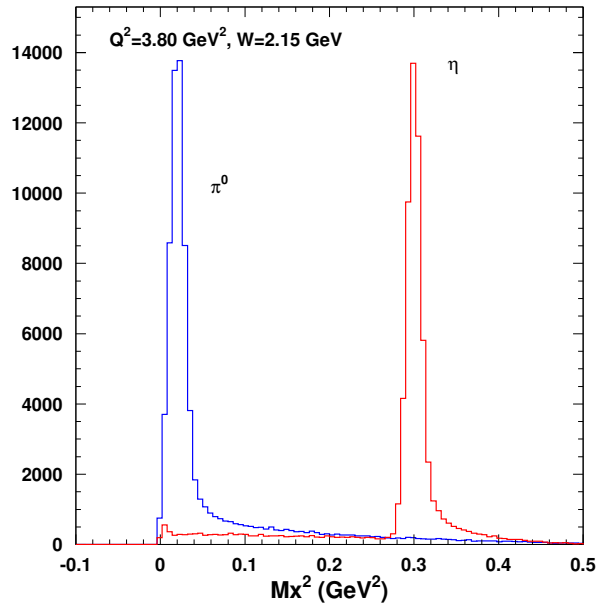

FIG. 6: *Simulated missing mass spectrum for Q^2=3.8 GeV^2 and W=2.0 GeV including both $(\vec{e}, e', \vec{p})\pi^0$ and $(\vec{e}, e', \vec{p})\eta$ production mechanisms (hard photon contribution not shown). Note that the π^0 and η reaction channels are both accessible with the same HRS setting.*

GeV at the high and low Q^2 settings. With this resolution the π^0 and η production processes can be clearly separated by placing cuts on the missing mass.

The contribution of hard photons from the $(e, e'p)\gamma$ reaction is a little more challenging and requires a full background subtraction. This is necessary since the reconstructed photon mass peak is smeared out under the reconstructed π^0 mass peak as illustrated in Figure 7. In the analysis we will use a combined fit to the missing photon and the missing π^0 mass peaks similar to the one done in the analysis of CLAS DVCS data [36]. Note that this subtraction method will be more reliable due to the better resolution of the two high resolution magnetic spectrometers in Hall A. In addition, the presence of the η missing mass peak allows for checks of the simulated π^0 missing mass resolution. Another possibility to check the missing mass resolution is the use of elastic scattering, which we are planning to take for at least some of the kinematic settings.

In order to estimate the hard photon contribution we have simulated the acceptance for both reactions using a Monte Carlo program. The photon cross section was approximated by the Bethe-Heitler contribution and the π^0 cross section was calculated from the average of the VGG and VGL predictions (longitudinal) and the transverse and interference components were calculated using the VGL model prediction. However, note that the interference terms are suppressed in the parallel kinematics used here. In Figure 7, the π^0 is denoted by the dashed crve and the photon is denoted by the dashed-dotted curve. Both curves are normalized by the phase space and scaled relative

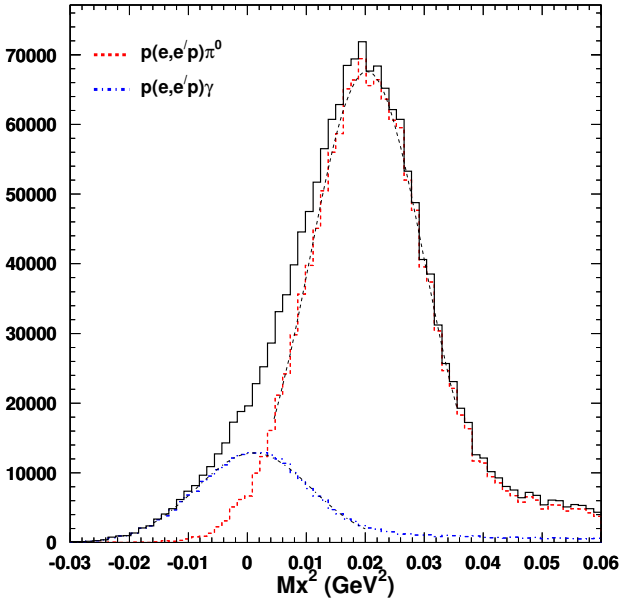

FIG. 7: *Simulated missing mass squared distribution for Q^2=3.8 GeV^2 and W=2.0 GeV including for the $p(e,e',p)\pi^0$ and the $p(e,e'\gamma)p$ production mechanisms.*

TABLE III: *The Bethe-Heitler component of the $p(e,e'\gamma)p$ cross section (dashed-dotted) and the $p(e,e',p)\pi^0$ (dashed) as calculated using the nominal assumptions for the π^0 rate calculations. Note that in the parallel kinematics used here, the LT and TT contributions are suppressed, leading to the relatively small Bethe-Heitler contribution listed below. The solid line represents the summed missing mass distribution.*

Q^2 (GeV^2)	x	t_{min} (GeV/c)^2	$\frac{d^5\sigma_{BH}}{d\Omega_e dE_e d\Omega_p}$ (pb/GeV/sr)	$\frac{\sigma^5_{\pi^0}}{d\Omega_e dE_e d\Omega_p}$ (pb/GeV/sr)
2.45	0.47	0.314	278	1200
2.00	0.50	0.372	202	750
2.00	0.55	0.494	115	610

to each other using the respective model cross section. The five-fold cross sections are listed in Table III. The result shown in Figure 7 is consistent with an independent study done using the Hall B Monte Carlo generator for exclusive π^0 and η production developed for the analysis of e16 data [37].

The measured background will be subtracted bin-by-bin from the azimuthal dependence of the asymmetry in the FPP. We expect a relatively little effect on the final uncertainty.

Besides providing information for the hard photon background subtraction, the exclusive η reaction channel provides additional physics content. In general, the comparison of the π^0 and η

TABLE IV: *Estimated background singles and accidental coincidence rates assuming a 10-cm hydrogen target and 100μ A electron beam. The accidental coincidence rate is calculated assuming a 2 ns coincidence timing gate. Note that the π^+, K^+ and proton accidental rates are the raw rates not including any PID. Including particle identification (as will be done in the offline analysis), the accidental rate reduces to a few percent of the real rate. The online π^- rejection rate in the electron arm is assumed to be 1:100.*

W (GeV)	Q^2 (GeV^2)	ϵ	$R_{\pi+}$ (kHz)	R_{K+} (kHz)	R_p (kHz)	$R_{\pi-}$ (kHz)	R_{e-} (kHz)	R_{acc} (Hz)	R_{real} (Hz)
1.90	2.45	0.77	139	11	70	0.3	2.8	1.2	1.0
2.00	3.10	0.65	178	14	83	0.3	0.9	0.5	0.4
2.00	3.80	0.42	212	17	98	0.2	0.2	0.1	0.1

cross sections as a function of Q^2 allows for model-independent flavor relation tests, and provides a way to probe the physics of spontaneous chiral symmetry breaking.

We have chosen a liquid hydrogen target with a length of 10 cm. This means that the target end windows will be in the acceptance of both spectrometers in all configurations and background subtractions are necessary. Background events from the target end windows will be measured using "empty" target data. The Hall A empty target consists of two thin Aluminium pieces separated by a length equivalent to the cryogenic target length [35]. However, the empty target is thicker by a factor of approximately ten relative to the target cell walls. The thicker target allows for a more rapid accumulation of counts for this background measurement. Assuming a maximum current of 30μA and 100 μA for the empty and cryo targets respectively results in a background measurement faster by a factor of 4. Based on previous measurements in Hall A, we estimate the aluminium background to be on the order of 1% for a 10-cm target. Therefore, a 20% measurement of the background requires an additional 30 minutes to acquire data for all kinematic settings.

D. Systematic Uncertainties

There are two primary sources of systematic error: uncertainties associated with the definition of the kinematics for each event and the uncertainties associated with the experimental apparatus (e.g. target thickness, analyzing power of the FPP etc.). In parallel kinematics each polarization component corresponds to a single response function, so that the influence of kinematic uncertainties like the beam energy and electron scattering kinematics is relatively small. The data are taken in parallel kinematics, so that instrumental uncertainties in the polarization observables are negligible to first order.

The Hall A spectrometers provide a momentum resolution of 3×10^{-4} in both the incident and scattered electron energies and an angular resolution of 1 mrad [35]. Simulations have been done using the standard Hall C Monte Carlo SIMC, which was modified to include the Hall A

TABLE V: *Estimated systematic uncertainties for the π^0 unseparated cross section.*

Source	Systematic Error (%)
Acceptance	2.0
Tracking efficiency	1.0
Trigger efficiency	1.0
Target thickness	1.0
Electronic deadtime	0.5
Kinematics	1.0
Charge	0.5
PID	1.0
Proton Absorption	2.0
Radiative Corrections	2.0
Total	4.2

spectrometers [44]. This code averages a physics model over the finite acceptance of the experimental spectrometers including the effect of offsets and final resolution. Shown in Figure 6 is the missing mass acceptance and resolution for the Q^2=3.80 GeV^2 measurement. In all simulations we assumed that the momenta are known to 3×10^{-4} and that angles were known to 1 mrad. The resulting resolution is reasonable and a cut on the pion peak separates backgrounds from other reaction channels like p$(e, e', p)\eta$ production.

The other main systematic effect results from the knowledge of the p-^{12}C analyzing power. All of the proton energies proposed for this experiment are < 800 MeV, so that the analyzing power database from LAMPF and TRIUMF is applicable. A global fit to the entire data set results in an uncertainty on $A_y(\theta)$ of $\pm$ 2%. Alternatively, we employ a parameterization of recent Hall A data taken in the low proton energy range proposed for this experiment.

The systematic uncertainties on the unseparated cross sections are estimated from previous cross section measurements in Hall A, and we expect to measure the unseparated cross section to 4.2%. Note that the final uncertainties on σ_L are dominated by the statistical uncertainty in the polarization components.

IV. PROJECTED ERROR AND TIME ESTIMATE

In preparing the count rate estimate we assume the following: 10-cm liquid hydrogen target thickness and 100 μA electron beam current, HRS solid angle and momentum bite of 6 msr and 5%, and $\approx$ 80% beam polarization. The dominant uncertainty in the beam time estimate are the statistical uncertainties in the recoil-polarization measurements and their propagation to those in the extracted longitudinal cross section. In addition, smaller systematic contributions due to the

polarimeter analyzing power, alignment and kinematic factors have to be taken into account.

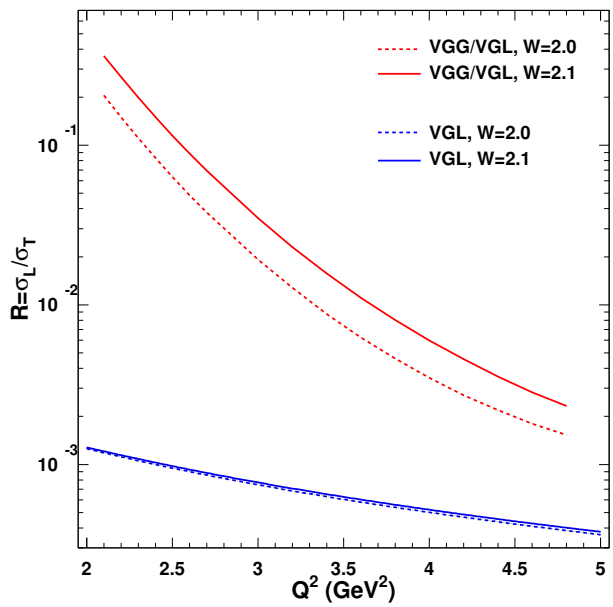

FIG. 8: *The Q^2 dependence of the longitudinal/transverse cross section ratio at t_{min}.*

The statistical uncertainty of a polarization component at the focal plane is given by [45]

$$dP_{FPP} = \sqrt{\frac{2}{N_0 \epsilon A_y^2}}, \tag{13}$$

where N_0 is the total number of events incident on the focal plane polarimeter, ϵ is the fraction of events that scatter successfully, and A_y^2 is the mean analyzing power. The polarimeter efficiency and analyzing power were estimated from a parameterization of recent Hall A data [39]. The statistical uncertainty in the individual recoil polarization components must take into account the spin precession through the spectrometer magnetic elements. For the longitudinal component one obtains, $dP_z \sim \frac{dP_{FPP}}{Sin\chi}$, where $\chi = \gamma(\mu_p - 1)(\theta_B)$ is the angle through which the proton spin precesses for a bending angle θ_B [38]. Here, γ is E_p/M_p and μ_p is the proton magnetic moment. For the HRS bending angle of Ω_B=45 degrees (for the central trajectory) and for the proton momenta proposed, this factor ranges between 0.974 and 0.999, thus results in rather small additional uncertainty in the measured polarization.

The uncertainty on the cross section ratio in the limit of small σ_L can be expressed,

$$dR \approx \frac{1}{h\epsilon\sqrt{1-\epsilon^2}}\, dP_{FPP}, \tag{14}$$

and the corresponding uncertainty on the longitudinal cross section is,

$$d\sigma_L \approx \sigma_0\, dR. \tag{15}$$

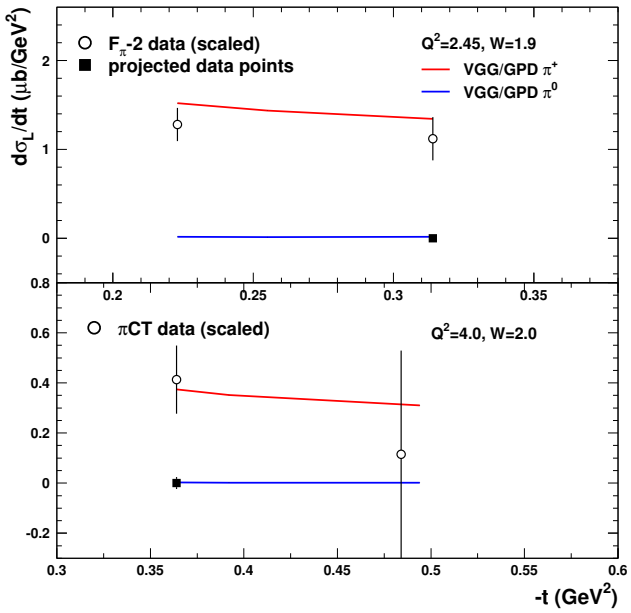

FIG. 9: *Projected uncertainties on the contribution of the longitudinal contribution to the π^0 cross section for the proposed kinematics (filled symbols) as predicted by the average of VGG/GPD and VGL/Regge model. The error bars indicate the absolute uncertainty. The open symbols denote the results for similar $-t$-bins from the recent F_π-2 [23] and [p]CT [25] measurements in Hall C. The two curves indicate the GPD/VGG prediction for both π^+ and π^0 production.*

The absolute size of the longitudinal π^0 cross section is effectively unknown above the resonance region and the theoretical model uncertainty in the relative size of σ_L and σ_T spans at least one order of magnitude. The longitudinal cross section as predicted in the VGL/Regge model for Q^2=2.45 GeV^2 is on the order of 0.1 nb/GeV^2 resulting in L/T ratios of $\approx 10^{-3}$. This ratio becomes even smaller as Q^2 increases (see Figure 8) making Rosenbluth separations difficult due to the unfavorable error propagation with two different acceptances. Predictions based on the VGG/GPD model predict a longitudinal cross section larger by a factor of 100, which gives a L/T ratio of $\approx$0.07. Recent data from Hall A present unseparated cross sections, which combined with the VGL or VGG predictions may hint that the longitudinal contribution may be larger than anticipated in either model. However, one has to be careful applying either model directly to the data due to the lack of knowledge of the longitudinal contribution to the π^0 cross section. For example, separated π^+ at Q^2=2.45 GeV^2 from F$_\pi$-2 suggests that even at t_{min}, where the pole contribution is maximal, the L/T ratio is still only equal. Thus, although the longitudinal π^0 cross section is certainly smaller, almost no information is available on the relative longitudinal contribution. The polarization recoil techniques offers an alternative to separate a small quantity like σ_L without the adverse increased sensitivity to the L/T ratio.

For the rate estimates we chose to estimate the size of the longitudinal cross section from the average value of the VGL/Regge and VGG/GPD cross section prediction at θ_{pq}=0 (in the lab frame). The VGL prediction does a relatively good job describing the recent unseparated Hall A data, though the $-t$-dependence has to be investigated further on both experimental and theoretical fronts. The VGL/Regge prediction was used for σ_T, σ_{LT} and σ_{TT}. For our kinematics, the cross section ratio as predicted by the average result from the VGL/Regge and the VGG/GPD models varies between 0.01 and 0.02 for virtual photon polarizations ranging between 0.56 and 0.77.

To illustrate the sensitivity of the experiment the projected uncertainties the two values of $-t_{min}$ and the Q^2-dependence of the longitudinal contribution to the π^0 cross sections are shown in Figure 9 and Figure 10. The filled symbols indicate the proposed π^0 measurement and the open symbols denote π^+ cross section data scaled to t_{min} for similar kinematics. The uncertainties on the proposed points have been estimated using the VGL/Regge model for both longitudinal and transverse cross sections assuming a systematic uncertainty of 4.2% in the unseparated cross section, beam polarization of 80% and statistical uncertainties on the polarization observables as listed in Table VI.

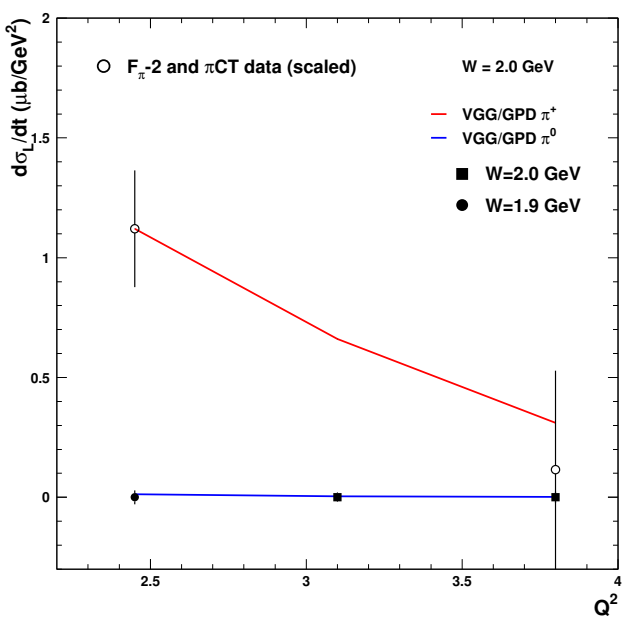

FIG. 10: *Projected uncertainties for the Q^2 dependence of the longitudinal π^0 cross section at fixed W (filled symbols). The open symbols denote data for overlapping $-t$-bins from the recent measurements in Hall C*

Our total time request is for 17 days of data, but additional time ($\approx$ 1 day) will be needed for calibration purposes and configuration changes. For example:

TABLE VI: *Beam time estimates assuming 100 μA on a 10-cm LH2 target, $d\sigma_0$=4.2% and h=80%.*

W (GeV)	Q^2 (GeV^2)	ϵ	N_0	dP_z	dR	hours
1.90	2.45	0.77	220k	0.036	0.092	106
2.00	3.10	0.65	200k	0.028	0.070	154
2.00	3.80	0.56	250k	0.028	0.076	145
Dummy						0.5
Total						406 (16.9 days)

- $H(e,e')$p elastic data for proton absorption measurement and spectrometer calibration $\approx$ 8 hours
- 14 spectrometer momentum changes requiring $\approx$ 30-60 minutes each
- 14 spectrometer angle changes requiring $\approx$ 30 minutes each
- FPP and optics calibrations requiring $\approx$ 8 hours
- Beam polarization measurement requiring $\approx$ 4 hours

The experiment will use a single beam energy of 5.75 GeV and the standard 10-cm cryogenic hydrogen target.

V. SUMMARY

In summary, we propose measurements of the p$(\vec{e},e',\vec{p})\pi^0$ reaction from which the longitudinal cross section will be separated via recoil polarization observables. The measurement will place a constraint on the contribution of non-pole processes to the pion electroproduction mechanism, which may influence the kinematics proposed for the 12 GeV F_π measurement. The measured π^0 and η cross sections will provide important information for the interpretation of existing and future Hall A and Hall B data, and may contribute to the 12 GeV π^0/η program. The experimental method has been successfully used in previous measurements in Hall A. All equipment needed for this experiment is existing and is standard Hall A equipment.

[1] C.E. Carlson and J. Milana, Phys. Rev. Lett **65**, 1717-1720 (1990).

[2] C.J. Bebek et al., Phys. Rev. **D13**, 25 (1976); Phys. Rev. **D17**, 1693 (1978).

[3] L. Mankiewicz, G. Piller, and T. Weigl, Eur. Phys. J. **C5**, 119 (1998).

[4] L. Mankiewicz, G. Piller and A. Radyushkin, Eur. Phys. J. **C10**, 307-312 (1999).

[5] M. Vanderhaeghen, M. Guidal and J.-M. Laget, Phys. Rev. **C57**, 1454 (1998); Nucl. Phys. **A627** 645 (1997).

[6] M. Vanderhaeghen, P.A.M Guichon, and M. Guidal, Phys. Rev. **D60**, 094017 (1999).

[7] T. Horn et al., Phys. Rev. Lett., **97**, 192001 (2006).

[8] A. Radyushkin, hep-ph/0101225, (2001).

[9] K. Goeke, M.V. Polyakov, and M. Vanderhaeghen, Prog. Part. Nucl. Phys. **47**, 401-515 (2001).

[10] L. Mankiewicz, G. Piller, and T. Weigl, Eur. Phys. J. **C5**, 119 (1998).

[11] M. Vanderhaeghen, P.A.M Guichon, and M. Guidal, Phys. Rev. Lett. **80**, 5064 (1998).

[12] L.L. Frankfurt, A. Freund, and M. Strikman, Phys. Rev. **D60**, 014010 (1999).

[13] M.I. Eides, L.L. Frankfurt, and M.I. Strikman, Phys. Rev. **D59**, 114025 (1999).

[14] J.C. Collins, L.L. Frankfurt, and M.I. Strikman, Phys. Rev. **D56**, 2982 (1997).

[15] D. de Florian, O.A. Sampayo and R. Sassot, Phys. Rev. **D57**, 5811 (1998).

[16] Y. Roblin and F. Sabatie, Deeply Virtual Compton Scattering at 6 GeV, proposal to Jefferson Lab PAC18.

[17] K. Joo, M. Ungaro, C. Weiss, V. Kubarovsky and P. Stoler, Hard Exclusive Electroproduction of π^0 and η with CLAS12, JLab 12 GeV Proposal PR12-06-101, 2006.

[18] J.J. Kelly et al., Phys. Rev. Lett. **95**, 102001 (2005); nucl-ex/0509004.

[19] G. Laveissiere et al., Phys. Rev. **C69**, 045203 (2004).

[20] T. Pospischil et al., Eur. Phys. J. **A12**, 125 (2001).

[21] C.N. Brown et al., Phys. Rev. Lett. **27**, 1611 (1971).

[22] D.J. Mack, H. Blok, and G. Huber, The Charged Pion Form Factor, TJNAF Proposal 93-021, 1993.

[23] D.J. Mack, H. Blok, and G. Huber, Extension to E93-021L: The Charged Pion Form Factor, TJNAF Proposal 01-004, 2001.

[24] J. Volmer et al., Phys. Rev. Lett., **86**, 1713 (2001).

[25] K.R. Garrow, D. Dutta and R. Ent, Measurement of Pion Transparency in Nuclei, TJNAF Proposal 01-107, 2001.

[26] J.-M. Laget, private communication (2006).

[27] G. Huber and D. Gaskell, Measurement of the Charged Pion Form Factor to High Q^2, JLab 12 GeV Proposal PR12-06-101, 2006.

[28] D. Drechsel and L. Tiator, J. Phys. **G18**, 449 (1992).

[29] H. Schmieden and L. Tiator, Eur. Phys. J. **A8**, 15-17 (2000).

[30] J.J. Kelly, Phys. Rev. **C60**, 054611 (1999).

[31] A.S. Raskin and T.W. Donelly, Ann. Phys. **191**,

[32] H. Schmieden, Eur. Phys. J. **A1**, 427 (1998).

[33] H.F. Jones, Nuevo Cimento **40**, 1018 (1965).

[34] R.L. Walker, Phys. Rev. **182**, 1729 (1969).

[35] J. Alcorn et al, Basic instrumentation for Hall A at Jefferson Lab, Nucl. Inst. Meth. **A522**, 294-346 (2004).

[36] S. Stepanyan et al., Phys. Rev. **87**, 182002 (2001).

[37] H. Avagyan, private communication (2006).

[38] V. Punjabi et al., Phys. Rev. **C71**, 055202 (2005).

[39] R. Gilman, private communication (2006).

[40] R. Gilman, A. Sarty and S. Strauch, Low Energy Deuteron Photodisintegration, proposal to Jefferson Lab PAC28.

[41] M.W. McNaughton et al., Nucl. Intrum. Meth. **A241**, 435 (1985).

[42] J. O'Connell and J. Lightbody, Comp. in Phys., May-June **57**, (1998).

[43] wiser.f by Steve Rock, Wiser fit of proton, pion and kaon cross sections.

[44] SIMC: Monte Carlo for Hall C, (2001).

[45] L. Pentchev, J. LeRose, and the FPP collaboration, Quadrupole alignment studies in the HRSs, JLab-TN-01-052. (2001).